Coulomb Four-Body Problem: Electron-Impact Double Ionization of Helium in the Threshold Regime

Xueguang Ren, Alexander Dorn, and Joachim Ullrich
Max-Planck-Institute for Nuclear Physics, 69117 Heidelberg, Germany
(Received 8 May 2008; published 29 August 2008)

Double ionization of helium by electron impact is studied in a kinematical complete experiment in the threshold regime at 5 eV excess energy. As expected the recoil ion carries the full initial projectile momentum and the emitted electrons' sum momentum in average is zero. The electron emission is revealed to be completely dominated by the symmetric 120° configuration predicted by many threshold theories but never observed experimentally before. Fully differential cross sections show a more complex structure than expected for a pure threshold collision dynamics.

DOI: 10.1103/PhysRevLett.101.093201 PACS numbers: 34.80.Dp

The dynamics of many-particle quantum systems is still one of the most important unsolved problems in quantum physics. A fundamental test system for the development of models is the breakup of an atom or molecule into a few charged particles. If these share only a small amount of energy and, thus, their mutual interaction energy is comparable to their kinetic energy this results in the complete breakdown of any independent particle or self-consistent field approximation [1], ubiquitous in atomic and molecular physics, strongly challenging theory.

Very close to the breakup threshold, the Wannier model [2] based on arguments from classical physics was able to predict some key features of the cross section for two-electron escape as, e.g., the energy dependence of the total cross section which generally is referred to as the Wannier threshold law. The main underlying principle of this approach is the identification of a stationary configuration where both electrons recede back-to-back from the residual ion and both experience at each point of their escape trajectory the same net force due to their mutual repulsion and the attraction by the ion. Since then this phenomenon has been under intense investigation (see Refs. [3,4] also summarizing earlier work). E.g., Rau [5] derived the Wannier threshold law based on quantum mechanical principles studying the Schrödinger equation for near-zero kinetic energies of both electrons. Klar and Schlecht [6] pioneered the extension of this treatment to systems with more particles, e.g., to three-electron escape as realized in triple-photoionization [the so-called $(\gamma, 3e)$ reaction] of lithium or electron-impact double ionization [the $(e, 3e)$ reaction] of helium. Following the Wannier approach their derivation is based on the assumption that the escape of several electrons from the ionic potential is only possible if their radial distances from the ion remain nearly equal. In addition, the minimization of the electrons' mutual repulsion results in particular angular configurations predicting, e.g., an equilateral triangle for three-electron escape. This is supported by calculations of differential cross sections 6 eV above the threshold applying the analytical 6*C* wave function [7] and more recently by the dynamical screened version (DS6*C*) of this wave function [8].

Emmanouilidou and Rost [9] performed semiclassical calculations for triple-photoionization of lithium. Surprisingly, in contradiction to the above-mentioned theories, they predict that the three electrons emerge in a *T*-shape pattern very close to threshold for excess energies down to at least $E_{\mathrm{exc}} = 0.5$ eV. In a detailed analysis of the semiclassical trajectories [10] it is concluded that the *T*-shaped configuration is the result of two different binary collision sequences. One electron of the 1*s* shell absorbs the primary photon close to the atomic nucleus and, on its way out, ''immediately'' interacts with the second 1*s* electron while the energy and momentum transfer to the to the third 2*s*-electron being ''further out'' occurs some 70 attoseconds later. Thus, in a recent extension of their study the authors argue for the $(\gamma, 3e)$ and the $(e, 3e)$ reactions that the three-electron emission pattern close to threshold strongly depends on the initial-state configuration of the bound electrons [11], being either *T*-shaped or an equilateral triangle. This result indeed is in disagreement to all earlier theoretical models for threshold ionization which postulate a target structure independent symmetric emission. Moreover, again in conflict with *all* other theories another, much earlier classical trajectory calculation [12] obtained a *T*-shape emission pattern for electron-impact double ionization of helium down to at least 2 eV above threshold and the symmetric configuration only at 0.5 eV excess energy.

Most experiments so far were restricted to the examination of the energy dependence of the total cross section, verifying the threshold law concerning the Wannier exponent and its energy range of validity. For noble gases this was done for electron-impact single and multiple ionization [13]. Good agreement with the Wannier power law was found for single and double ionization. On the other hand double-photoionization studies for lithium [14] and beryllium [15] revealed unexpected oscillations in the energy dependence of the cross section not predicted by the Wannier model but in excellent agreement with the

Coulomb-dipole law developed by Tempkin [16]. The different behavior compared with noble gases was attributed to the more loosely bound electrons in Li and Be. For triple-photoionization the threshold behavior of the cross section was found to be in agreement with the Wannier law for Li [17], Neon and Argon [18].

Kinematically complete threshold studies of the electron emission have been reported for two-electron escape, namely, for electron-impact single ionization and for photo double ionization. So far, respective experiments exploring the correlated emission of a pure three-electron system receding from the residual ion at low excess energy was performed for electron-impact double ionization of helium [19]. As will be discussed below, for 106 eV electron impact where the total cross section is $\sigma^{2+} \approx 2 \times 10^{-20}$ cm^2 and the excess energy amounts to $E_{\text{exc.}} =$ 27 eV the authors could demonstrate that the three final-state continuum electrons are strongly correlated and electron emission is only allowed for particular configurations. On the other hand the excess energy was still rather far above the double ionization threshold and, thus, the results can neither critically test available threshold theories nor resolve the above-mentioned controversy.

To settle the situation for this fundamental collision system we have performed new $(e, 3e)$ measurements at a projectile energy of $E_0 = 84$ eV, only 5 eV above the double ionization threshold of helium. The experimental challenge at this energy arises from the tiny total cross section of about 10^{-21} cm^2 being 5 orders of magnitude smaller than the single ionization cross section at the same energy [20].

The measurements were performed using a highly efficient reaction microscope. The setup has been described in detail elsewhere [21,22]. Briefly, a well-focused (1 mm), pulsed electron beam (pulse length $\approx$1.5 ns, repetition rate 180 kHz, $\approx 10^4$ electrons/pulse), produced by a standard thermocathode gun, crosses and ionizes the helium gas target (2 mm diameter, 10^{12} atoms/cm^3), a three-stage supersonic gas jet. Using parallel electric (0.7 V/cm) and magnetic (5 G) fields, the fragments in the final state are projected onto two-dimensional position- and time-sensitive multihit detectors equipped with delay-line readout. In this way a large part of the full solid angle is covered, 100% for the detection of the recoil-ion and 80% for the electrons. From the positions of the hits and the time of flight, the vector momenta of the detected particles can be reconstructed. The complete collision kinematics was obtained by detecting the momentum vectors of two outgoing electrons and the recoiling doubly charged ion in a triple coincidence. The third electron momentum then was calculated exploiting momentum conservation. From collision events where all final-state particles happened to be recorded in a quadruple coincidence their momentum sum revealed the experimental momentum resolution along the different directions in space. Thus, the recoil-ion momentum resolution (full width at half maximum-FWHM) is 0.3 a.u. for the transversal and 0.15 for the longitudinal direction. For all the emitted electrons, the transversal (longitudinal) momentum resolution is better than 0.1 a.u. (0.05 a.u.).

The kinematics for fragmentation close to the threshold strongly differs from the situation at high impact energies since the projectile loses most of its kinetic energy. Then, all three final continuum electrons share the residual excess energy E_{exc}, which can be written as

$$E_{\text{exc}} = E_0 - \text{IP} = E_1 + E_2 + E_3.$$

Here $E_{1,2,3}$ denote the energies of the three final-state electrons, respectively, and IP is the double-ionization potential (IP = 79 eV). The recoil-ion energy can be safely neglected, due to its large mass. On the other hand, momentum conservation forces the final-state particles to share the initial momentum $|\vec{p}_0| = p_0 = \sqrt{2E_0}$ by virtue of

$$\vec{p}_0 = \vec{p}_1 + \vec{p}_2 + \vec{p}_3 + \vec{p}_{\text{ion}} = \vec{p}_{\text{sum}} + \vec{p}_{\text{ion}}.$$

$\vec{p}_{\text{sum}}$ is the sum momentum of all three final-state electrons. For the present measurement at $E_0 = 84$ eV ($p_0 =$ 2.5 a.u.) as well as for the previous one at $E_0 = 106$ eV ($p_0 = 2.8$ a.u.) none of the three electrons has an energy higher than $E_{\text{exc}} = 5$ eV and 27 eV and, thus, cannot carry more than $p_i = 0.6$ a.u. and 1.4 a.u., respectively. Therefore, in order to fulfill momentum conservation, a large fraction of the initial momentum has to be transferred to the recoil ion. This should be even reinforced by the observation of Dürr *et al.* [19] that due to their mutual repulsion the final-state electrons are emitted with large relative angles partially compensating their momenta. This expectation is nicely confirmed by the final-state distribution of the recoil-ion He^{2+} momentum and the respective sum momentum of the three electrons $\vec{p}_{\text{sum}}$ shown in Fig. 1. For $E_{\text{exc}} = 27$ eV ($p_0 = 2.8$ a.u.) in Fig. 1(a) $\vec{p}_{\text{sum}}$ is scattered around zero with the maximum of the distribution slightly shifted towards the projectile forward direction around 0.4 a.u. On the other hand the ion momentum is peaked at $p_z \approx 2.4$ a.u. coming close to the projectile momentum. The spread of the distributions is consistent with the maximum momentum a final-state electron can gain ($p_i \leq 1.4$ a.u.). Approaching threshold at $E_{\text{exc}} =$ 5 eV [$p_0 = 2.5$ a.u., Fig. 1(b)] the kinematics becomes significantly more restricted. The electron sum momentum now is perfectly centered within the experimental uncertainty of ± 0.02 a.u. at zero momentum and the recoil-ion momentum distribution is located right at the projectile momentum of 2.5 a.u. Again, the now reduced spread of the distributions is in accordance with the maximum electron momentum of $p_i \leq 0.6$ a.u. These observations are consistent with the expectation that at higher projectile energy one of the electrons preferentially carries a larger part of the excess energy and is emitted more towards the forward direction shifting $\vec{p}_{\text{sum}}$ accordingly. Very differently at the low excess energy, the information on the direction of the projectile as well as its identity is com-

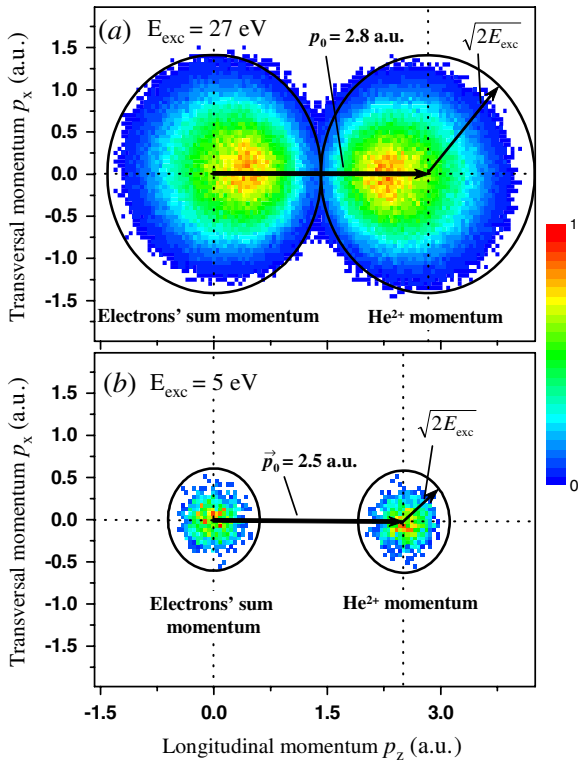

FIG. 1 (color online). The distribution of the final-state electrons' sum momentum p_{sum} and the respective recoil-ion momentum distribution projected onto a plane containing the incoming beam direction (indicated). (a) For the projectile energy $E_0 = 106$ eV ($p_0 = 2.8$ a.u.). (b) For $E_0 = 84$ eV ($p_0 = 2.5$ a.u.). The incoming projectile momentum $\boldsymbol{p}_0$ is indicated. The limiting momentum ranges for the case that one electron carries the full excess energy are marked by circles.

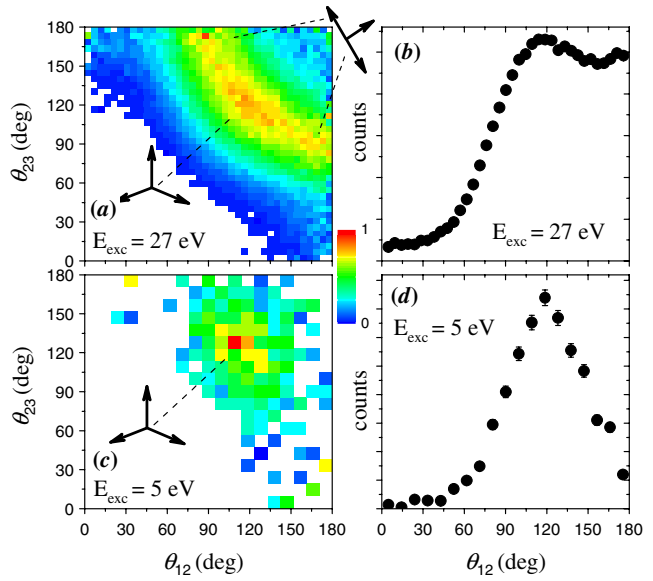

FIG. 2 (color online). Cross section differential in the relative emission angles of the final-state electrons. Left diagrams: Cross section as a function of θ_{12} and θ_{23} (see text). (a) For $E_0 = 106$ eV ($E_{\mathrm{exc}} = 27$ eV). (b) For $E_0 = 84$ eV ($E_{\mathrm{exc}} = 5$ eV). In this representation the solid angle correction factor $(\sin\theta_{12} \times \sin\theta_{23})^{-1}$ was applied and gives rise to an increased data scattering along the boundaries of the diagrams. Right diagrams: Cross section summed over θ_{23}. (b) For $E_0 = 106$ eV, (d) For $E_0 = 84$ eV.

pletely lost and, thus, not apparent at all in the electron sum momentum distribution. This is a strong indication that for $E_0 = 84$ eV indeed the threshold regime has been reached. In previous experimental studies the energy range where the threshold law is valid could be established only by measuring the total cross section dependence as a function of the excess energy. Such triple electron escape measurements for electron-impact double ionization of helium [13] and triple-photoionization of neon, oxygen [23], and lithium [14] have shown that the threshold laws seem to be valid up to about 5 eV above the threshold or even more.

The triple-escape angular correlations between the final-state continuum electrons are shown in Fig. 2(c), where the cross section is plotted as a function of their relative emission angles. While θ_{12} is the angle in between the momentum vectors of two arbitrarily chosen final-state electrons e_1 and e_2, θ_{23} is the respective angle enclosed by e_2 and the residual electron e_3. The diagram contains all double ionization events recorded, regardless of how the excess energy is shared among the electrons or into which direction the electrons are emitted with respect to the incoming beam. For comparison, we have also shown the previous results obtained for $E_0 = 106$ eV impact energy taken from [19] in Fig. 2(a). This representation clearly reflects the strong angular correlation between the three final-state continuum electrons. While small relative angles are completely suppressed there is a long ridge of allowed configurations ranging from the back-to-back emission of two electrons with the third one perpendicular to the symmetric 120° configuration in the middle of the diagram. Proceeding to the lower excess energy of 5 eV [Fig. 2(c)] the range of allowed configurations is found to be decisively further reduced. The T-shape configuration is strongly suppressed and three-electron emission is allowed only in the vicinity of the symmetric 120° configuration. This is revealed in Figs. 2(b) and 2(d) even more clearly where the cross section is shown as a function of the emission angle θ_{12} of any two electrons while integrating over θ_{23}. Whereas at $E_{\mathrm{exc}} = 27$ eV two maxima at $\theta_{12} = 120°$ and 180° are present, representing the symmetric and the T-shape emission, respectively, the latter one has disappeared completely at $E_{\mathrm{exc}} = 5$ eV and only the 120° maximum remains.

Therefore the present experiment unambiguously confirms theoretical models predicting this threshold configuration [6–8,11] and, simultaneously, falsifies the early classical trajectory calculations [12] which obtained a T-shape emission down to 2 eV excess energy.

Finally, in Fig. 3 fully differential cross sections (FDCS) are presented for equal energy sharing $E_1 = E_2 = E_3 = 1.6$ eV $\pm$ 1 eV among the final-state electrons and for the

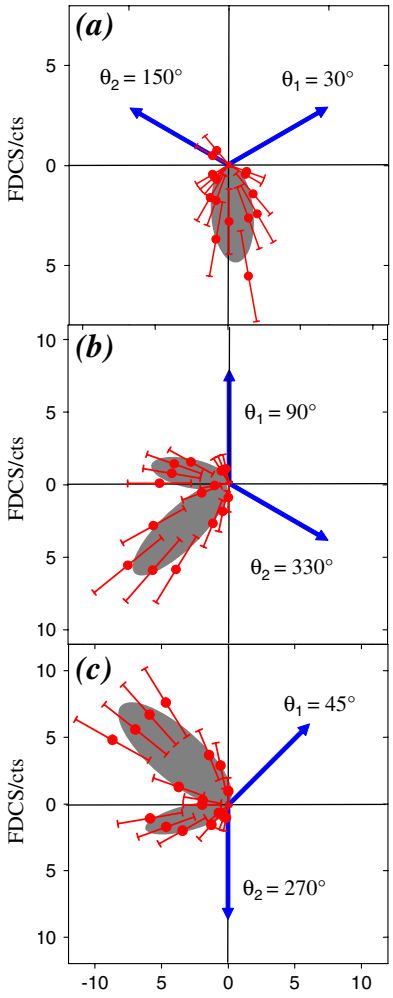

FIG. 3 (color online). Fully differential cross sections for symmetric energy sharing $E_1 = E_2 = E_3 = 1.6$ eV $\pm$ 1 eV among the final-state electrons. All three outgoing electron momentum vectors are in a common plane containing the incoming electron beam axis $\boldsymbol{p}_0$ (indicated as an arrow). Two-electron emission angles are fixed along the directions indicated by arrows. The gray lobes are meant for guiding the eye.

coplanar scattering geometry where the emitted electrons are ejected in a common plane ($\pm 20°$) containing the incoming projectile direction. The cross sections are plotted for three different emission angle combinations of two electrons (as indicated by arrows in the diagrams) as a function of the third electron's ejection angle θ_3. It again becomes obvious that due to the electron-electron repulsion the third electron is emitted only with large relative angle to each one of the other two which is consistent with the cross section plot in Fig. 2(c) discussed above. In panel (a) two electrons are fixed at 120° relative angle ($\theta_1 = 30° \pm 20°$, $\theta_2 = 150° \pm 20°$) and, accordingly, the maximum cross section of the third electron is observed at $\theta_3 \approx 270°$ where symmetric emission occurs. In diagrams (b) and (c) one electron is fixed perpendicular to the projectile axis [270° and 90°, in (b) and (c), respectively] with the other being forward emitted (45° and 330°, respectively). Surprisingly, the cross section pattern displays not just a single lobe as in (a) but also two maxima separated by a significant minimum close to 180°. This nontrivial structure demonstrates that the three-electron escape reaction is considerably more involved than it would be expected from the pure electron-electron repulsion just minimizing threshold dynamics and giving rise to symmetric 120° emission. Therefore, adequate theories for this collision system are urgently required since calculations simply modeling the postcollision interaction of the electrons definitely will fail to reproduce the observed structures.

In conclusion a kinematically complete experiment for electron impact double ionization of helium at 5 eV excess energy has been performed. The fact that the recoil ion carries all the momentum of the projectile indicates that the threshold regime has been reached. For the first time a pure symmetric triangular breakup geometry is observed as predicted by several threshold theories. Finally, FDCS for equal energy sharing are presented showing a more complicated structure than expected at this low excess energy.

[1] J. M. Feagin and R. D. Filipczyk, Phys. Rev. Lett. **64**, 384 (1990).
[2] G. H. Wannier, Phys. Rev. **90**, 817 (1953); **100**, 1180 (1955).
[3] J. M. Rost, Phys. Rev. Lett. **72**, 1998 (1994).
[4] J. Macek and H. Yu. Ovchinnikov, Phys. Rev. A **54**, 544 (1996).
[5] R. Rau, Phys. Rev. A **4**, 207 (1971).
[6] H. Klar and W. Schlecht, J. Phys. B **9**, 1699 (1976).
[7] A. Malcherek and J. S. Briggs, J. Phys. B **30**, 4419 (1997).
[8] J. R. Götz, M. Walter, and J. S. Briggs, J. Phys. B **39**, 4365 (2006).
[9] A. Emmanouilidou and J. M. Rost, J. Phys. B **39**, 4037 (2006).
[10] A. Emmanouilidou and J. M. Rost, Phys. Rev. A **75**, 022712 (2007).
[11] A. Emmanouilidou, P. Wang, and J. M. Rost, Phys. Rev. Lett. **100**, 063002 (2008).
[12] M. S. Dimitrijević and P. Grujić, J. Phys. B **14**, 1663 (1981).
[13] S. Denifl *et al.*, J. Phys. B **35**, 4685 (2002).
[14] R. Wehlitz *et al.*, Phys. Rev. Lett. **89**, 093002 (2002).
[15] R. Wehlitz *et al.*, Phys. Rev. Lett. **93**, 023003 (2004).
[16] A. Tempkin, Phys. Rev. Lett. **49**, 365 (1982).
[17] R. Wehlitz *et al.*, Phys. Rev. A **61**, 030704(R) (2000).
[18] J. B. Bluett *et al.*, Phys. Rev. A **69**, 042717 (2004).
[19] M. Dürr *et al.*, Phys. Rev. Lett. **98**, 193201 (2007).
[20] M. S. Shah *et al.*, J. Phys. B **21**, 2751 (1988).
[21] J. Ullrich *et al.*, Rep. Prog. Phys. **66**, 1463 (2003).
[22] M. Dürr *et al.*, Phys. Rev. A **75**, 062708 (2007).
[23] J. A. R. Samson and G. C. Angel, Phys. Rev. Lett. **61**, 1584 (1988).